

Eur. J. Inorg. Chem. **2017** · ISSN 1099–0682

<https://doi.org/10.1002/ejic.201700983>

SUPPORTING INFORMATION

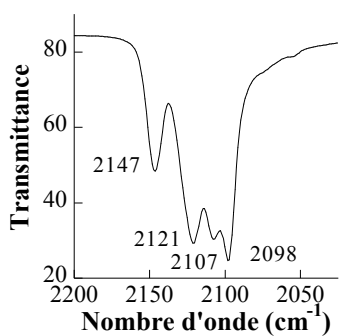
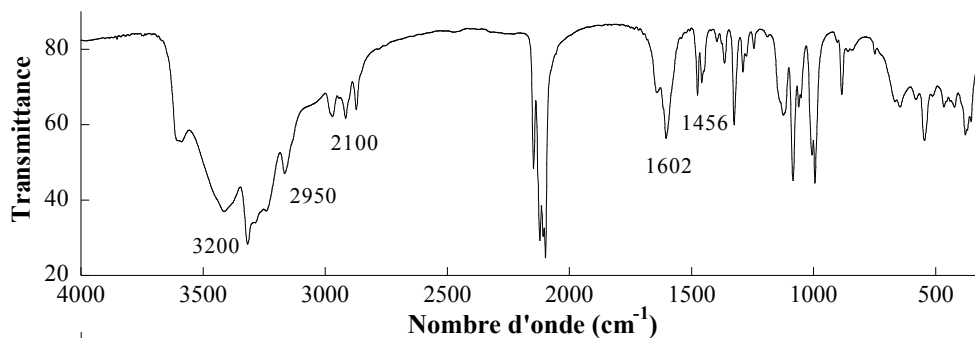
Title: Direct Evidence of a Photoinduced Electron Transfer in Diluted “Molybdenum-Copper” Molecular Compounds

Author(s): Nathalie Bridonneau, Pierre Quatremare, Hans Jurgen von Bardeleben, Jean-Louis Cantin, Sébastien Pillet, El-Eulmi Bendeif, Valérie Marvaud*

1. Infra-red Spectra
2. Crystallographic data
3. XRD under irradiation
4. Photomagnetic measurements
5. EPR spectroscopy measurements

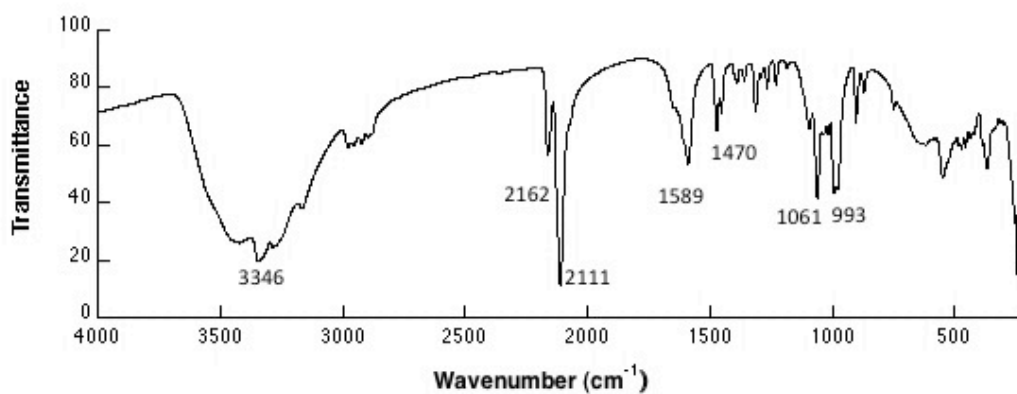
1. Infrared Spectra

Infrared Spectra of $\text{MoZn}_2\text{-tren}$ (**1**)



Nombre d'onde	Attribution
1456	CH_2
1602	N-H
2098,2107	Mo-CN
2121,2147	Mo-CN-Zn
2950	C-H
3200	N-H

Infrared Spectra of $\text{Mo}(\text{Zn}_{0.95}\text{Cu}_{0.05})_2\text{-tren}$ (**4**)



2. Crystallographic data

The crystal structure of the pure Zn compound **1** has been reported in our previous study (Bridonneau *et al.*, *Chemical Communications* **2015**, 51, (39), 8229).

Single crystal X-ray diffraction data were collected on complex **5**: Mo(Zn_{0.9}Cu_{0.1})₂-tren using a Microfocus Supernova diffractometer equipped with a two dimensional ATLAS detector, using Mo K α radiation ($\lambda = 0.71073 \text{ \AA}$), and a Helijet He open flow cryosystem. The temperature was fixed at 10 K. Diffraction data were first collected at 10 K in the ground state (GS) using ω -scans. The unit cell determination and data reduction were performed using the *CrysAlis* program suite (Oxford Diffraction, 2012) on the full data set. The corresponding unit cell parameters are $a = 14.7573(5) \text{ \AA}$, $b = 14.8266(4) \text{ \AA}$ and $c = 30.9111(9) \text{ \AA}$ with a cell volume of $V = 6763.3(3) \text{ \AA}^3$. 98894 reflections were measured up to a maximum resolution of $\theta_{\text{max}} = 33.00^\circ$, and merged to 23348 unique reflections ($R_{\text{int}} = 0.0677$). Numerical absorption correction was performed. The corresponding structure was solved in the $Pca2_1$ space group by direct methods with the SHELXS-2014 program (Sheldrick, 2014) and refined on F^2 by weighted full matrix least-squares methods using the SHELXL-2014 program (Sheldrick, 2014). All non-hydrogen atoms were refined anisotropically, hydrogen atoms were generated at their ideal position and treated using a riding model, constraining the isotropic displacement parameters to 1.2 times those of the attached C atom. Hydrogen atoms of water molecules were not located in difference Fourier maps. Before irradiation, the residual electronic density map does not show any significant peak (Fig. S1), especially in the neighborhood of the Mo2-C10-N10-Cu4/Zn4 fragment, which is the most affected by irradiation (*vide-supra*). Selected structural parameters are given in table S1.

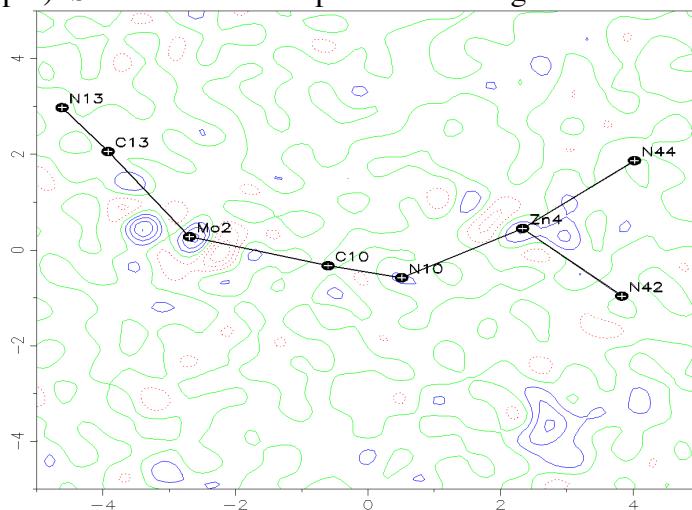


Figure S1: Residual electronic density map of the fundamental state of **5** in the Mo2-C10-N10-Cu4/Zn4 fragment (positive contours in blue, negative in red).

Interatomic distances (Å)	Mo(Zn) ₂ -tren	Mo(Zn _{0.9} Cu _{0.1}) ₂ -tren
Mo1-C	2.135(3)-2.165(4)	2.136(6)-2.162(5)
Mo2-C	2.152(3)-2.182(4)	2.149(6)-2.170(6)
free C-N	1.147(4)-1.165(4)	1.140(8)-1.169(7)
Zn/Cu-N(tren)	2.035(3)-2.285(3)	2.037(4)-2.247(5)
Zn/Cu-N(cyano)	2.050(3)-2.105(3)	2.031(6)-2.092(5)
Mo1...Mo2	10.0981(4)	10.6987(8)
Zn1/Cu1...Zn2/Cu2	6.4885(6)	6.4823(9)
Zn3/Cu3...Zn4/Cu4	6.4469(6)	6.4157(9)
Mo1...(Zn1/Cu1,Zn2/Cu2)	5.2431(4)-5.0692(5)	5.2184(8)-5.0596(8)
Mo2...(Zn3/Cu3,Zn4/Cu4)	5.3246(4)-5.0383(5)	5.3020(8)-5.0271(8)
Angles (°)	Mo(Zn) ₂ -tren	Mo(Zn _{0.9} Cu _{0.1}) ₂ -tren
Mo1-C-N(cyano)	175.6(3)-178.5(3)	175.5(5)-178.0(5)
Mo1-C-N(free)	175.1(3)-178.7(3)	174.4(5)-178.6(5)
Mo2-C-N(cyano)	176.8(3)-177.5(3)	176.8(5)-177.3(5)
Mo2-C-N(free)	176.8(3)-178.0(3)	176.8(5)-178.4(5)
C-N-Zn1/Cu1	157.1(3)	157.9(6)
C-N-Zn2/Cu2	145.3(3)	145.6(5)
C-N-Zn3/Cu3	165.0(3)	165.8(5)
C-N-Zn4/Cu4	137.1(3)	137.5(5)
C1-Mo1-C2	77.90(14)	78.0(2)
C9-Mo2-C10	75.12(12)	74.7(2)

Table S1: Table of main distances and angles of Mo(Zn)₂-tren complex (**1**) [Mo(CN)₆ {(μ -CN)Zn₂C₆H₁₈N₄}₂](H₂O)₁₀ (Bridonneau *et al.*, *Chemical Communications* **2015**, 51, (39), 8229) and Mo(Zn_{0.9}Cu_{0.1})₂-tren complex (**5**) [Mo(CN)₆ {(μ -CN)Zn_{0.9}Cu_{0.1}C₆H₁₈N₄}₂](H₂O)₁₀ in the ground state (10K)

[Mo ^{IV} (CN) ₈]	(APBC-8) D_{4d}	(DD-8) D_{2d}
Mo2	0.21839	2.46492
Mo1	0.46628	1.70948

Table S2: Distorsion of the coordination polyhedron of octacyanomolybdate centers in **1**

3. XRD under irradiation

A single crystal was irradiated at 10K with a diode laser at 405 nm ($P = 70$ mW) during 60 min. Diffraction data were then collected on the irradiated sample. 98894 reflections were measured up to a maximum resolution of $\theta_{\max}=30^\circ$, and merged to 23348 unique reflections ($R_{\text{int}} = 0.0677$). Numerical absorption correction was performed.

Photo difference maps

Photo-difference maps have been calculated for visualisation of the light-induced changes in electron density, and identification of the related structural changes from the GS to the excited state (Fig. S1). Common independent reflections between the GS and photo-irradiated state have been used to compute the experimental X-ray photo-difference map by Fourier transform of the difference ($F_{\text{photo-irradiated}}^{\text{obs}}(hkl) - F_{\text{GS}}^{\text{obs}}(hkl)$), using the structure factor phases from the GS structural refinement. The calculated photo-difference map reveals some structural reorganisation. For the Mo1 molecule, this map displays electron deficient regions (red coloured) centred on the position of the heaviest atoms in the ground state (Mo1, Zn2, Zn1), and an electron density accumulations (blue coloured) around Mo1. This corresponds mainly to an increase of atomic displacement parameters (atomic disorder) in the photo-irradiated state. On the contrary, for the second molecule, the map highlights a slight displacement of the Mo2 and Zn4/Cu4 atoms in the photo-irradiated state, as evidenced by electron deficient regions (red coloured) centred on the position of the atoms together with adjacent electron density accumulations (blue coloured) not centred on the atomic position.

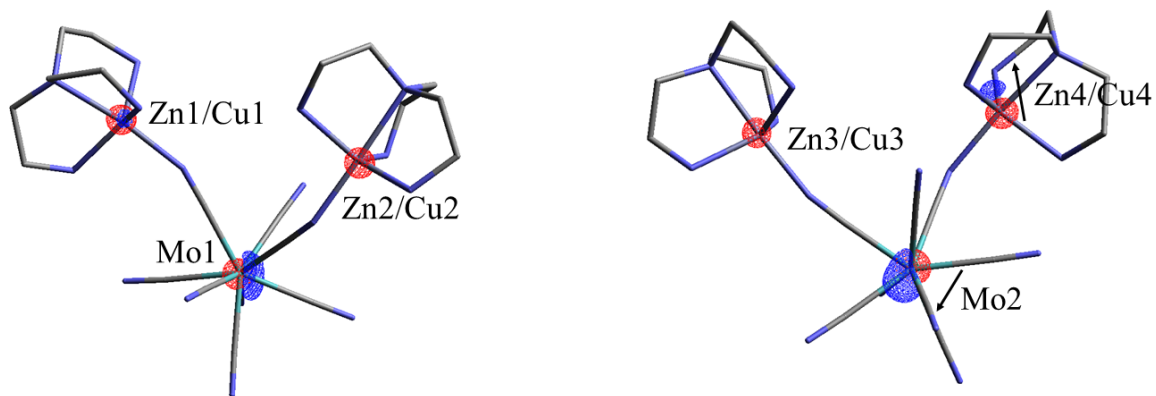


Figure S2: 3D photo-difference map of 5 with isosurface of $\pm 6.0 \text{ e}\text{\AA}^{-3}$ (red, negative; blue, positive) at 10 K after irradiation with 405 nm. Arrows indicate the putative atomic displacement in the photo-irradiated state.

Structural refinement of the photo-irradiated state

The photo-irradiated state crystal corresponds to a superposition of different molecular species located at approximately the same position in the unit cell: ground state of [MoZn₂], [MoZnCu] and [MoCu₂] species, and photo-excited state of [MoZn₂], [MoZnCu] and [MoCu₂] species. It is impossible to deconvolute all these structures with the present photo-crystallographic data. We performed a structural refinement considering only one molecular configuration, without adding any constraints, so that the refined atomic positions correspond to an average position over the possible different molecular species (ground state and excite state) in the crystal. We compare in figure S3 the ORTEP plots of the refined ground state, and photo-irradiated state structures.

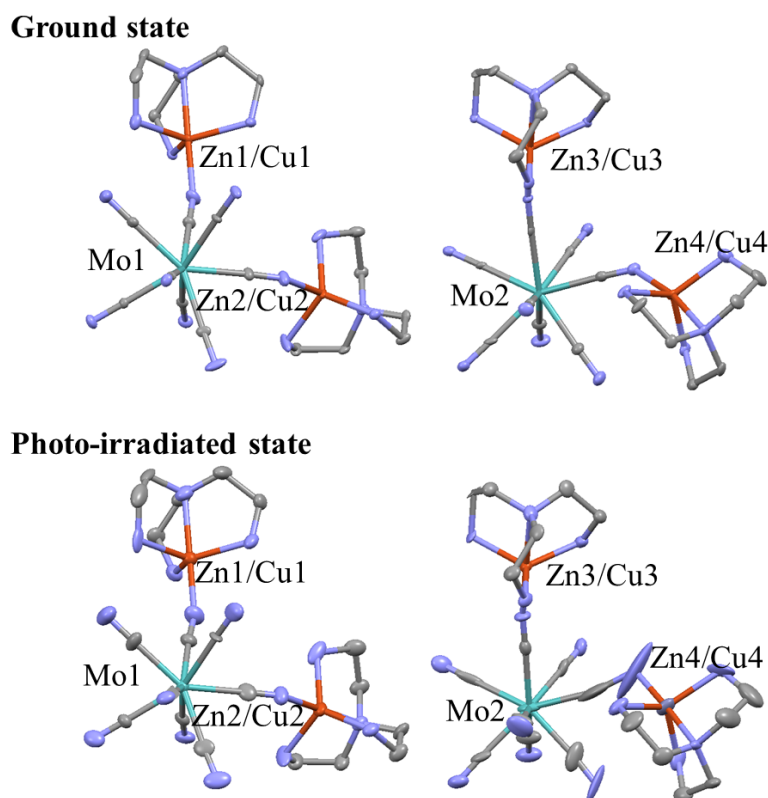


Figure S3. (top) ORTEP plot of the ground state refined crystal structure of **5**, (bottom) ORTEP plot of the ground state refined crystal structure of **5**.

	Ground state	Photo-irradiated state (60 min)
T/K	10	10
Crystal System	orthorhombic	orthorhombic
Space group	Pca21	Pca21
a / Å	14.7573(5)	14.8462(5)
b / Å	14.8266(4)	14.9542(5)
c / Å	30.9111(9)	30.9058(10)
V / Å ³	6763.3(3)	6861.5(4)
Z	8	8
Measured data	98894	55059
Θ_{\max}	32.996	26.370
R_{int}	0.0677	0.0624
μ / mm^{-1}	1.811	1.785
Tmin / Tmax	0.624 / 0.702	0.624 / 0.702
Independent data	23348	12574
R1 [$F^2 > 2s(F^2)$]	0.0581 [0.0467]	0.0733 [0.0653]
wR2 [$F^2 > 2s(F^2)$]	0.1073 [0.0997]	0.1786 [0.1717]

Table S3: Crystallographic data and refinement details of **5**

4. Photomagnetic measurements

Compound 4 ($\text{Mo}(\text{Zn}_{0.95}\text{Cu}_{0.05})_2\text{-tren}$)

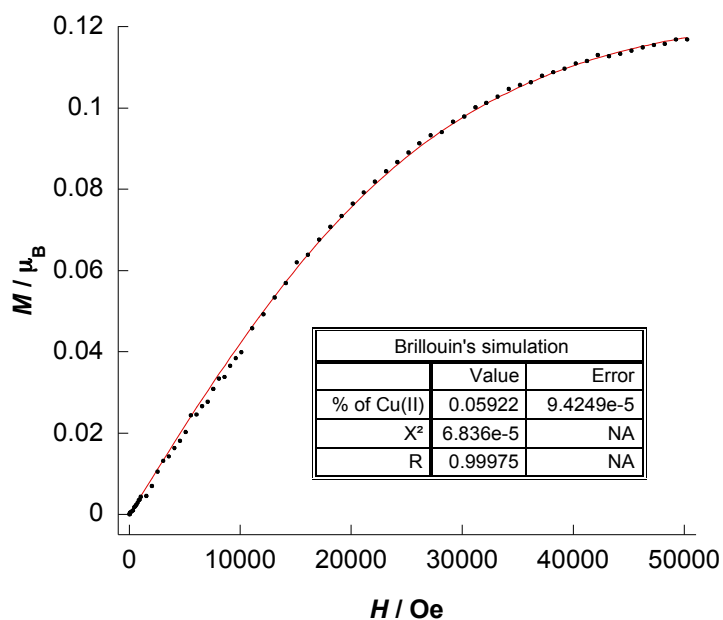


Figure S4: Magnetization (M) vs Field (H) curve at 2K for **4** ($\text{Mo}(\text{Zn}_{0.95}\text{Cu}_{0.05})_2\text{-tren}$) and Brillouin's simulation

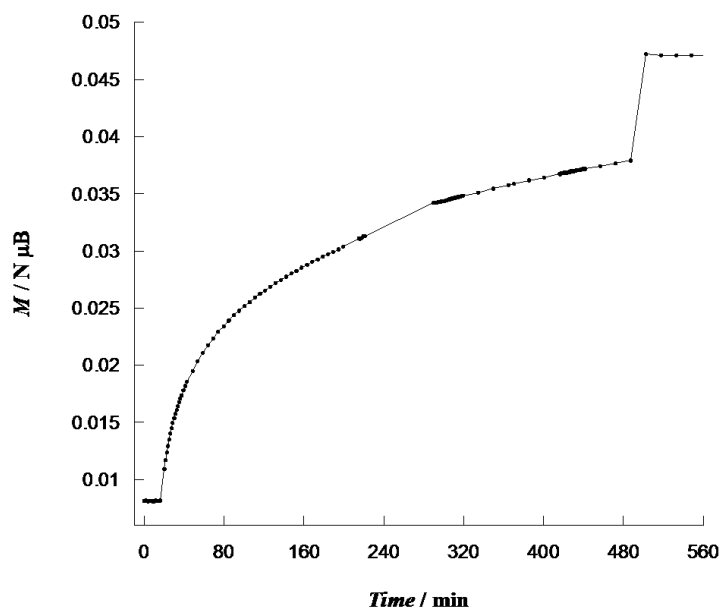


Figure S5: Evolution of the magnetization of **4** upon light irradiation (at 500 min., light is switch off)

Compound 5 ($\text{Mo}(\text{Zn}_{0,9}\text{Cu}_{0,1})_2\text{-tren}$)

Photomagnetic measurements for compound **5**

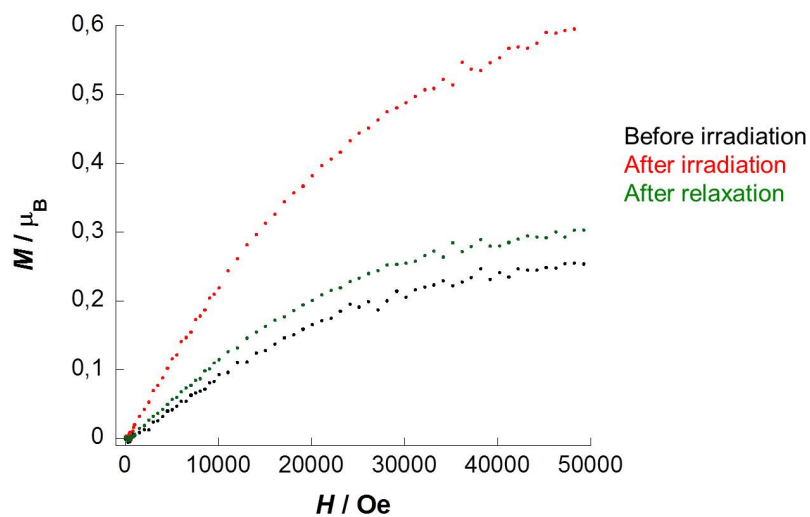


Figure S6: Magnetization (M) vs Field (H) curve at 2K for **5** before irradiation (black curve), after irradiation (red curve) and after relaxation (green curve)

Comparison of the magnetic data in relation with copper percentage

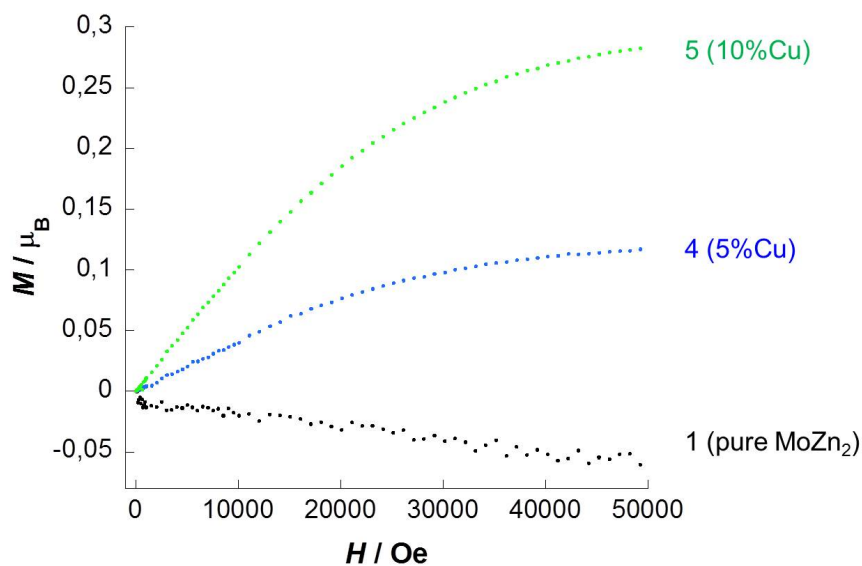


Figure S7: Comparison of the magnetization vs field curves at 2K for compounds **1**, **4** and **5**

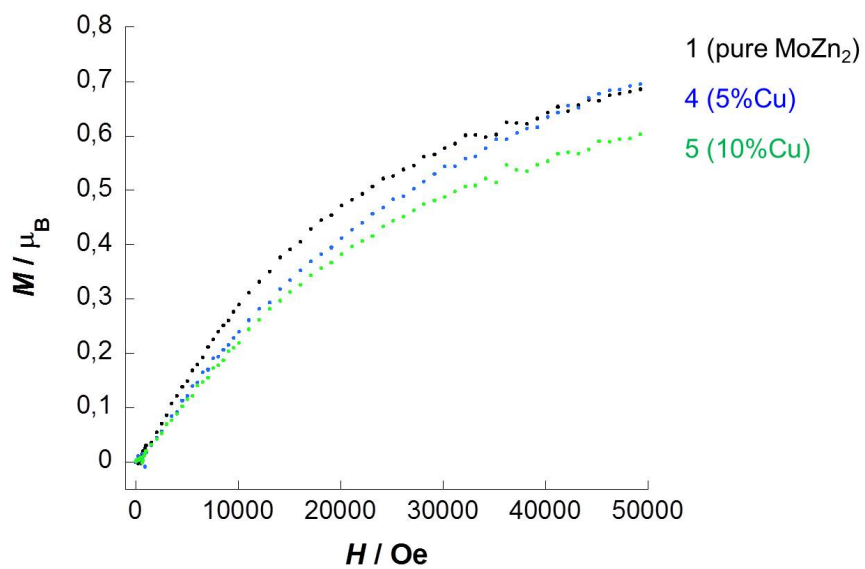


Figure S8: Comparison of the magnetization vs field curves at 2K obtained after irradiation for compounds **1**, **4** and **5**

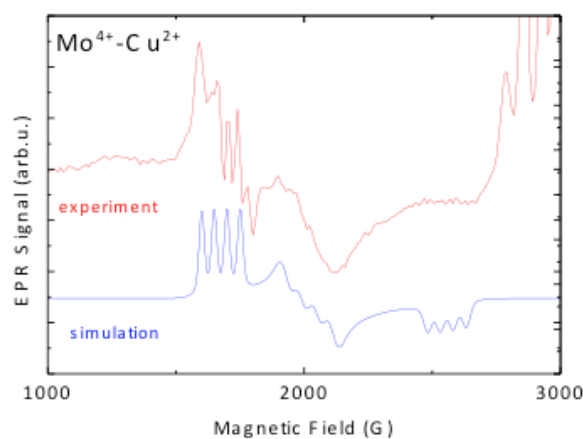
5. EPR spectroscopy measurements

EPR measurements were performed on polycrystals with a commercial Bruker X-band spectrometer and a 4–300 K variable temperature cryostat, which allowed in-situ photoexcitation. The magnetic field modulation frequency was set at 100 kHz and the modulation amplitude and the microwave power were both adjusted to avoid saturation. The spectra were measured at temperatures between 4 K and 300 K. The excitation of the samples at low temperature was performed with a diode laser at 405nm and an Ar ion laser at 488 nm. Typical laser power 100mW.

The polycrystalline samples showed well-resolved EPR spectra with partially resolved hyperfine structure. The samples were sufficiently polycrystalline not to introduce a significant anisotropy in the EPR spectra. Analysis and simulation of the EPR spectra were performed with the Bruker Simfonia powder spectrum simulation program.

As usual for spin $S=3/2$ centers with large zero field splitting relative to the Zeeman interaction, the spectrum simulation were performed with an effective spin $S_{\text{eff}}=1/2$.

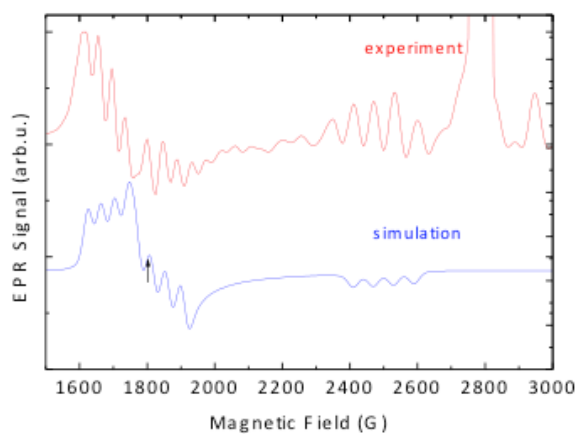
Compound 3 ($\text{Mo}(\text{Zn}_{0.99}\text{Cu}_{0.01})_2\text{-tren}$)



Simulation

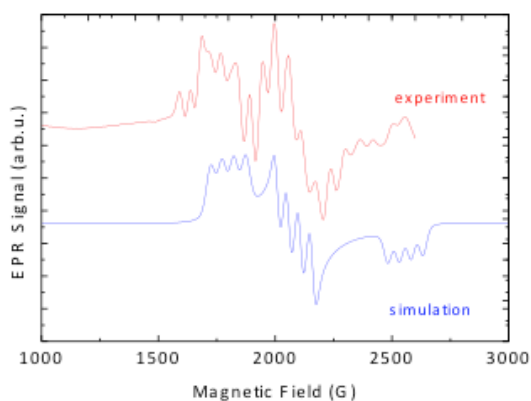
$S_{\text{eff}}=1/2$	$g_x=3.98$	$A_x=50\text{G}$	$\Delta B_x=20\text{G}$
	$g_y=3.30$	$A_y=60\text{G}$	$\Delta B_y=45\text{G}$
	$g_z=2.61$	$A_z=50\text{G}$	$\Delta B_z=30\text{G}$

Figure S9: experimental and simulated EPR spectra of Mo(IV-HS)-Cu(II), for compound **3**; the simulation parameters: g -factors, Cu HF interaction parameters and the linewidth are given above



simulation	$S_{\text{eff}}=1/2$	$g_x=3.96$	$A_x=40\text{G}$	$\Delta B_x=25\text{G}$
		$g_y=3.62$	$A_y=45\text{G}$	$\Delta B_y=25\text{G}$
		$g_z=2.67$	$A_z=60\text{G}$	$\Delta B_z=30\text{G}$

Figure S10: Theoretical and experimental EPR spectra of Mo(IV-HS)-Cu(II), for compounds **3**; the simulation parameters: g-factors, Cu HF interaction parameters and the linewidth are given above



simulation	$S_{\text{eff}}=1/2$	$g_x=3.71$	$A_x=50\text{G}$	$\Delta B_x=35\text{G}$
		$g_y=3.20$	$A_y=50\text{G}$	$\Delta B_y=25\text{G}$
		$g_z=2.61$	$A_z=50\text{G}$	$\Delta B_z=30\text{G}$

Figure S11: Theoretical and experimental EPR spectra of Mo(IV-HS)-Cu(II), for compounds **4**; the simulation parameters: g-factors, Cu HF interaction parameters and the linewidth are given above